
DINCON´ 2007
6th Brazilian Conference on Dynamics, Control and Their Applications
IBILCE - UNESP
S. J. Rio Preto, SP
Brazil
May 22- 25, 2007
Proceedings of the 6th Brazilian Conference on Dynamics, Control and Their Applications
ISBN: 978-85-85769-32-1

SP 10729

AGRICULTURAL X-RAY TOMOGRAPHY BASED ON WAVELETS AND PARALLEL ARCHITECTURE OF DSP PROCESSORS

Paulo E. Cruvinel
Embrapa Agricultural Instrumentation, São Carlos, Brazil, cruvinel@cnpdia.embrapa.br

Abstract: The use of computerized X-ray tomography and its related instrumentation has been diversified and recently has been also encountered in works related to soil physics. This work presents a platform based on wavelets and Digital Signal Processors (DSPs) for tomographic image reconstruction. Results show the suitability of the method, which allows not only a better signal to noise ratio for image reconstruction procedures but also regarding to a significant performance gains in relationship to the time demanded for image reconstruction and visualization.

Keywords: X-ray tomography, Wavelets, DSP.

1. INTRODUCTION

X-ray tomography was primarily used for medical diagnosis, however today its applications have been diversified, including recently soil physics and other agricultural applications [1][2][3][4].

The basis of transmission X-ray tomography are related with a narrow beam of monoenergetic photons with energy E and an incident photon flux intensity N_0 that passes through a path p of a non-homogeneous absorber of thickness x (in cm), leading to an emerging photon intensity N given by:

$$N = N_0 e^{\oint_p (-\mu(\rho, Z_N, E)x)dp} \quad (1)$$

where μ (in cm^{-1}) is correlated to the material of physical density ρ (in g/cm^3) and atomic number Z_N. The attenuation coefficient, as a function of the X-ray energy, can be decomposed into contributions from the modes of photon interaction with matter and its total is given by:

$$\mu_{tot} = \mu_{ph} + \mu_C + \mu_R + \mu_p \quad (2)$$

where each term of Eqn (2) is related to the mode of photon interaction i.e., photoelectric effect, Compton scattering, Rayleight scattering, and pair production respectively [5].

Although linear attenuation coefficients are convenient for engineering applications and shielding calculations, they are proportional to the density of the absorber, which depends on the physical state of the material. Since molecular binding energies are smaller than the energies involved in X-ray radiography and tomography, it is reasonable approximations to assume that linear attenuation coefficient is directly proportional to the physical density and write:

$$N = N_0 e^{\oint_p (-(\frac{\mu(Z_N, E)}{\rho})\rho x)dp} \quad (3)$$

where μ/ρ (in cm^2/g) is the mass attenuation coefficient. If the absorber is a chemical compound or mixture, its mass attenuation coefficient can be approximately evaluated from the coefficients for the constituent elements according to the weighted sum:

$$\frac{\mu}{\rho} = \sum_i w_i \left(\frac{\mu_i}{\rho_i}\right) \quad (4)$$

where w_i is the proportion by weight of the ith constituent of the material. The mass attenuation coefficient of the compound or a mixture can be therefore, calculated from the mass attenuation coefficient of the components. It is important to observe that the differences in linear attenuation coefficient for different materials are dependent on the energy, which leads to the definition of the contrast of the computerized X-ray tomographic images. In addition, the quality of the images is correlated to both the hardware of the tomographic systems and their image reconstruction methods.

This work presents the development of a system to reconstruct X-ray tomographic images with the use of Wavelets and DSP processors.

2. MATERIALS AND METHODS

This development brought the implementation of parallel algorithms that permitted obtaining a high performance level in processing by utilizing DSP processor characteristics. Utilized in the parallel reconstruction modules were the tools Code Composer from *Texas Instruments*, the *Borland Builder* C++ 5.0, as the development environment of the graphic interface and Parallel C language from 3L in the development of parallel tasks of 2D and 3D reconstruction.

To accomplish this study, phantoms and soil samples were utilized that were tested in the computerized minitomograph scanner for agricultural applications installed in *Embrapa Instrumentation Center* in the city of Sao Carlos, Brazil [6].

In the conventional platforms, the tomographic projections are processed utilizing the CPU from a PC-Computer. Since this study has all of the necessary calculations for the reconstruction of tomographic slices, the data filtration and the interpolation for the three-dimensional reconstruction planes are directed to be processed by DSP processors in parallel platform, leaving the PC-Computer processor to only do graphic interface tasks processing, communicate with the root DSP processor to access the hard disk and to visualize two -dimensional and three-dimensional images. Fig. 1 presents the structure of the DSP architecture based on the TMS320C40 to optimize the performance of tomographic images reconstruction.

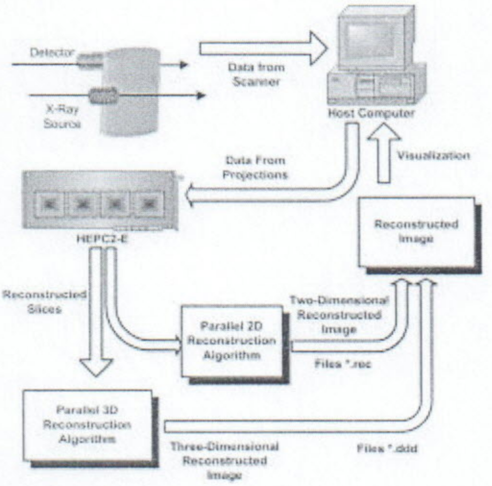

Fig. 1 - DSP structure based on the TMS320C40.

In this research it was used the TIM-40 module of HET40EX model manufactured by *Hunt Engineering*. The modules TIM-40 follow the *Texas* standard called *Texas Instruments Module* (TIM) that has a standard module size following the defined module specifications [7].

The reconstruction algorithm was based on the back-projection of the projections, with base on both the Fourier sections theorem and Radon transform. This theory established that the Fourier transform of the projection of an image g(x, y) taking the angle θ as equivalent to a piece of the two-dimensional transformation of g(x, y). In other words, the Fourier transform of $P_\theta(t)$ supplies the values of $G(?_1, ?_2)$.

The way to facilitate the visualization of this development of back projected filtered reconstruction was to separate them in two different equations. The first is to filter the projection data for each angle θ, as follows:

$$Q_\theta(t) = \int_{-\infty}^{\infty} S_\theta(\omega)|\omega| e^{j\omega t} d\omega \qquad (5)$$

where $S_\theta(\omega)$ represents the Fourier transform of the convoluted projections with a filter in a frequency domain. After the filtered projections are back projected to obtain an object function, given by:

$$g(x,y) = \int_0^{\pi} Q_\theta(x\cos\theta + y\,\mathrm{sen}\,\theta)d\theta \qquad (6)$$

where each component represents a pixel of coordinates (x,y) in the reconstructed image g(x,y). In a distinguishing manner, the discrete filtered back-projection is represented by:

$$\hat{\bar{g}}(x,y) = \frac{\pi}{K}\sum_{i=1}^{K} Q_\theta(x\cos\theta_i + y\,\mathrm{sen}\,\theta_i) \qquad (7)$$

where K angles θ_i are the discrete values of θ for each $P_\theta(t)$ known [8].

Additionally, for three-dimensional reconstruction we have used polynomial B-spline wavelets to interpolate planes between the 2D reconstructed slices. Fig. 2 illustrates the basis used to reach such arrangement.

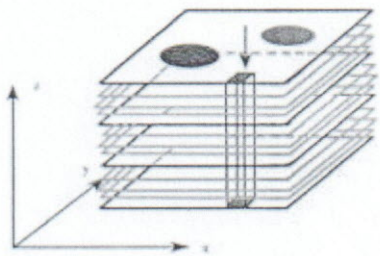

Fig. 2 – Arrangement for 3D image reconstruction.

An admissible wavelet function ψ satisfies at least two essential properties. First, it must be included in the finer resolution approximation space. Specifically, this means that the function ψ(x/2) is a polynomial spline of order n and it can be represented by its B-spline expansion as:

$$\psi(x/2) = \sum_{k\in Z} s(k)\beta^n(x-k) \qquad (8)$$

Second, the wavelet must be orthogonal to the polynomial spline subspace at the same resolution level. This leads to the following constraint:

$$\forall k \in Z, \langle \psi(x/2), \beta^n(x/2-k)\rangle = \left[s * u_2^n * b^{2n+1}\right]_{\downarrow 2}(k) = 0 \qquad (9)$$

which explicit the representation of this inner product in terms of the discrete convolution operators. Up sampling by a factor of two and taking the ztransform is possible to write:

$$\frac{1}{2}\left(S(z)U_2^n(z)B_1^{2n+1}(z) + S(-z)B_1^{2n+1}(-z)\right) = 0 \qquad (10)$$

where $U_2^n(z)$ and $B_1^{2n+1}(z)$ are the z-transform of u_2^n and b^{2n+1}, respectively. Both u_2^n and b^{2n+1} are finite impulse response (FIR) operators. It can be verified by substitution that a particular solution of this equation is:

$$S(z) = zU_2^n(-z)B_1^{2n+1}(-z) \qquad (11)$$

This solution also corresponds to the sequence s of minimal length. Taking the inverse z-transform we obtain an explicit formula for the B-spline wavelet of order n, which is given by:

$$\beta_W^n(x/2) = \sum_{k=-\infty}^{+\infty} u_2^n * b^{2n+1}(k+1)\beta^n(x-k) \quad (12)$$

where $\beta_W^n(x/2)$ is the wavelet, and it generates all the wavelet spaces $W_{(i)}$. Hence, the set of functions $\left\{\beta_W^n(2^{-i}x-k),(i,k)\in Z^2\right\}$ is an unconditional basis of L_2. The wavelets are symmetrical functions that are shifted by one unit with respect to the standard B-spline functions [9]. The B-spline basis functions and wavelets are therefore good approximation of Gabor functions which are known to be maximally localized in both time and frequency.

Additionally, in the development of this tool was used the *OpenGL* library to develop the three-dimensional visualization interface.

3. RESULTS AND DISCUSSIONS

The manner to facilitate the implementation of the DSP parallel platform and become more modular was to develop five nuclei, that permitted the end user of the system complete use of the form of parallel architecture that was the most intuitive and thus became transparent to the end user of the DSP processor architecture. One can see, that measurements for performance evaluation can be obtained for the parallel modules, i.e., to study the efficiency and the system speed. Such measurements allowed both the improvement of the reconstruction algorithms and the optimization of the communication between processors.

The development of parallel algorithm utilizes the Manager-Worker model for distribution of tasks between processors. Like this, the root processor assumes the role of Manager, staying responsible for the distribution of tasks to the other processors, called Workers. At the system initiation, they require tasks for the Manager that are sent in as a portion of the work and as Worker processors they finally send their results to the Manager processor and return to more required work. The graphic interface permits the selection of the data files having projections that will be reconstructed through the three-dimensional and two-dimensional parallel algorithms. With these applications one can make a three-dimensional and two-dimensional visualization permitting the selection of the region of interest, using the gray-level (or pseudo-colors) tones to represent the linear attenuation coefficients encountered in an analyzed sample. Besides this, one can also choose the parameters of filtration, regions of interest, and one can determine the real planes sequence, and the qiantity of interpolated planes inside of each pair of real form planes to increase the quality of the three-dimensional object reconstructed. Fig. 3 shows the developed applications in Microsoft Windows®, which interface parallel modules for 2D and 3D reconstruction and 3D visualization, and results for a soil sample analysis with visualization and measurements of soil bulk density at 59.9 keV.

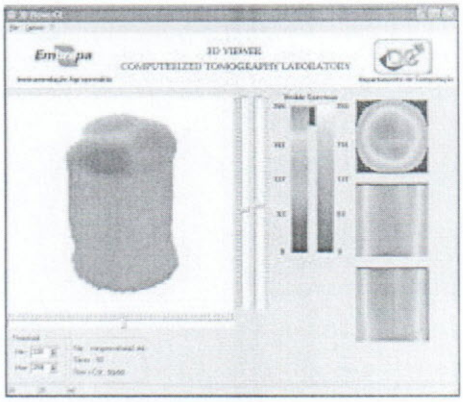

Fig. 3 – The interface for 2D and 3D image analysis.

Because of the communication algorithm based on the sending of data with greater granularity with better utilization of the processing power of the Worker processors the processing time was optimized. With this, one has to have a greater locality of Worker data processors and the smallest number of work requests for the Manager, making the communication cost fall substantially. In this way, the Manager and each Worker established only two communications during the tomographic reconstruction process. As a first part of the process the system determines the region that will be used for the Worker to reconstruct, and secondly is established the conversation between the two or more processors from which the Manager obtains a response. Fig. 4 shows the performance evaluation and results were achieved considering different configurations, i.e., with standard configuration and the parallel processor architecture.

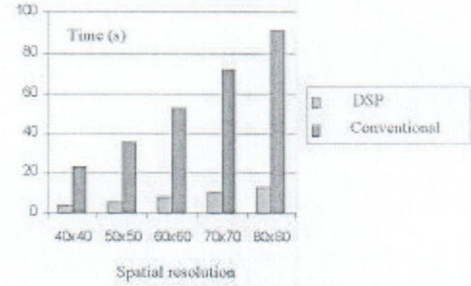

Fig. 4 – Performance evaluation.

4. CONCLUSION

The use of DSPs allowed significant gains in relationship to the time demanded with improvement in the performance to a factor of 6 for the reconstruction algorithm. Similarly, the system speedup maintained itself at nearly ideal, indicating a high degree of parallelism in the execution of tasks.

ACKNOWLEDGMENTS

The author expresses his appreciation to the National Council for Scientific and Technological Development (CNPq, Processes No. 300.704/82-8, and No. 141.369/02-7), as well as to Dr. Maurício F. L. Pereira for research

collaboration in the field of parallel computing, control and image processing.

REFERENCES

[1] G. M. Hounsfield, Brit J Radio, v 46, pp 1016-1022, 1973.
[2] A. M. Cormack, J. App. Phys, v. 34(9), pp 2722-2727, 1963.
[3] A. M. Petrovic, J. E. Siebert, P. E. Rieke, Soil Science Soc. Am. J, n.46, p.445-450, 1982.
[4] J. M. Hainsworth, LA. G. Aylmore, Aust. Journal Soil Res., n.21, p.1435-1443, 1983.
[5] S. Crestana, The Computerized Tomography as a new method for soil water content studies, São Carlos, USP, Doctoral Thesis, pp. 140,1986.
[6] A. Macedo, C.M.P. Vaz, J.C.D. Pereira, J.M. Naime, P.E. Cruvinel, S. Crestana, Inter. Jour. of the Biology, Chemistry, Physics and Technology of Wood, Holzforschung/Vol.56, pp. 535-540, 2002.
[7] TMS320C40 Data Sheet, Texas Instruments, 1-3, 1996.
[8] P.E. Cruvinel, R. Cesareo, S. Crestana, S. Mascarenhas, IEEE Transactions on Instrumentation and Measurement, v.39 No. 5, 1990.
[9] P. Lapsley, J. Bier, A. Shoham, E. A. Lee, Berkeley, California, 1996.